Lithos 248–251 (2016) 1–11

Contents lists available at ScienceDirect

Lithos

journal homepage: www.elsevier.com/locate/lithos

The significance of PGE variations with Sr–Nd isotopes and lithophile elements in the Emeishan flood basalt province from SW China to northern Vietnam

Chusi Li [a,b,*], Edward M. Ripley [b], Yan Tao [a], Ruizhong Hu [a]

[a] State Key Laboratory of Ore Deposit Geochemistry, Institute of Geochemistry, Chinese Academy of Sciences, Guiyang 550002, China
[b] Department of Geological Sciences, Indiana University, Bloomington, IN 47405, USA

ARTICLE INFO

Article history:
Received 7 September 2015
Accepted 29 December 2015
Available online 2 February 2016

Keywords:
Flood basalts
Picrites
Incompatible trace elements
Platinum-group elements
Sr–Nd isotopes
Mantle heterogeneity

ABSTRACT

New analyses of siderophile–lithophile elements and Sr–Nd isotopes in the Permian basalts and picrites from northern Vietnam, the southernmost occurrence of the Emeishan flood basalt province, together with previously published data, are used to address the question of whether any meaningful correlation between these elements and isotopes exists at a province scale. The available data show that negative correlations between ε_{Nd}, $(^{87}Sr/^{86}Sr)_i$ and mantle-normalized $(Nb/Th)_n$ are present in the basalts but not in the associated picrites. This indicates that crustal contamination is negligible in the picrites but significant in some of the basalts. The picrites and basalts from the entire province show negative correlations between $(Rh/Ru)_n$, $(Pt/Ru)_n$, $(Pd/Ru)_n$ and Mg-number. This indicates that Ru behaves compatibly whereas Rh, Pt and Pd behave incompatibly during magma differentiation. The incompatible behavior of Rh in natural basaltic systems is also supported by the fact that $(Pt/Rh)_n$ remains constant with decreasing Mg-number in the lavas. Depletions of Pd and Pt, and to a lesser degree Cu, in some basaltic samples characterized by relatively low ε_{Nd} and $(Nb/Th)_n$ support the notion that sulfide saturation in the magmas was triggered by a combination of siliceous crustal contamination and addition of external sulfur. Within the entire flood basalt province only the picrites from Song Da, northern Vietnam show clear depletion in Ir relative to Ru. These picrites are also characterized higher Al_2O_3/TiO_2 and lower mantle-normalized La/Yb (0.2–2.4) than those from elsewhere in the province, possibly due to the involvement of an Ir-depleted, fertile mantle component in magma generation at this location.

1. Introduction

The combination of radiogenic isotope ratios and variations in platinum-group element (PGE) concentrations is a potentially powerful tool in the evaluation of mantle sources for various mafic volcanic rocks ranging from basalts to komatiites. Sr and Nd isotope ratios have been utilized in the definition of mantle end-members (e.g., Zindler and Hart, 1986) and correlated trends define the "mantle array" (e.g., DePaolo and Wasserburg, 1976). These isotopic systems are also routinely utilized in the evaluation of crustal contamination processes that may affect mafic magmas (e.g., DePaolo, 1981). Platinum-group elements (PGE) have been used to evaluate core formation (e.g., Gaetani and Grove, 1997), mantle formation and differentiation (e.g., Lorand et al., 2008), and processes that may have affected the development of the continental lithosphere (Becker et al., 2006; Maier et al., 2012). The PGEs are highly chalcophile and hence high degree partial melts of the mantle are expected to exhaust some or all PGE-rich sulfide components of the mantle (Lorand et al., 2013; Luguet et al., 2007); for this reason komatiites typically contain high PGE concentrations (Barnes et al., 2015; Fiorentini et al., 2010). Basalts tend to have lower concentrations of PGEs, generally thought to be due to lower degrees of mantle melting and variable retention of immiscible sulfide liquid (e.g., Hamlyn and Keays, 1986; Mungall and Brenan, 2014). Fractional crystallization of high degree mantle melts produces positive trends between Mg-number and incompatible PGEs such as Pt and Pd. Because of the compatible behavior of Ir, Ru and Os in olivine and chromite (e.g., Brenan et al., 2012) fractional crystallization may result in these elements exhibiting negative trends with Mg-number. The utilization of radiogenic isotopes and PGE geochemistry offers the potential to evaluate petrologic linkages between various rock suites in a large igneous province and its potential for magmatic sulfide deposits (e.g., Jowitt and Ernst, 2013).

The ~260 Ma Emeishan flood basalt province covers an area of $>0.3 \times 10^6$ km^2 at the edge of the South China Block (Fig. 1). The flood basalts and picrites in the Song Da district, northern Vietnam are the southern extension of the Emeishan province. In this paper we use PGE concentrations, Sr and Nd isotope ratios, and lithophile trace

* Corresponding author at: Department of Geological Sciences, Indiana University, Bloomington, IN 47405, USA. Tel.: +1 812 855 1558.
E-mail address: cli@indiana.edu (C. Li).

http://dx.doi.org/10.1016/j.lithos.2015.12.027
0024-4937/

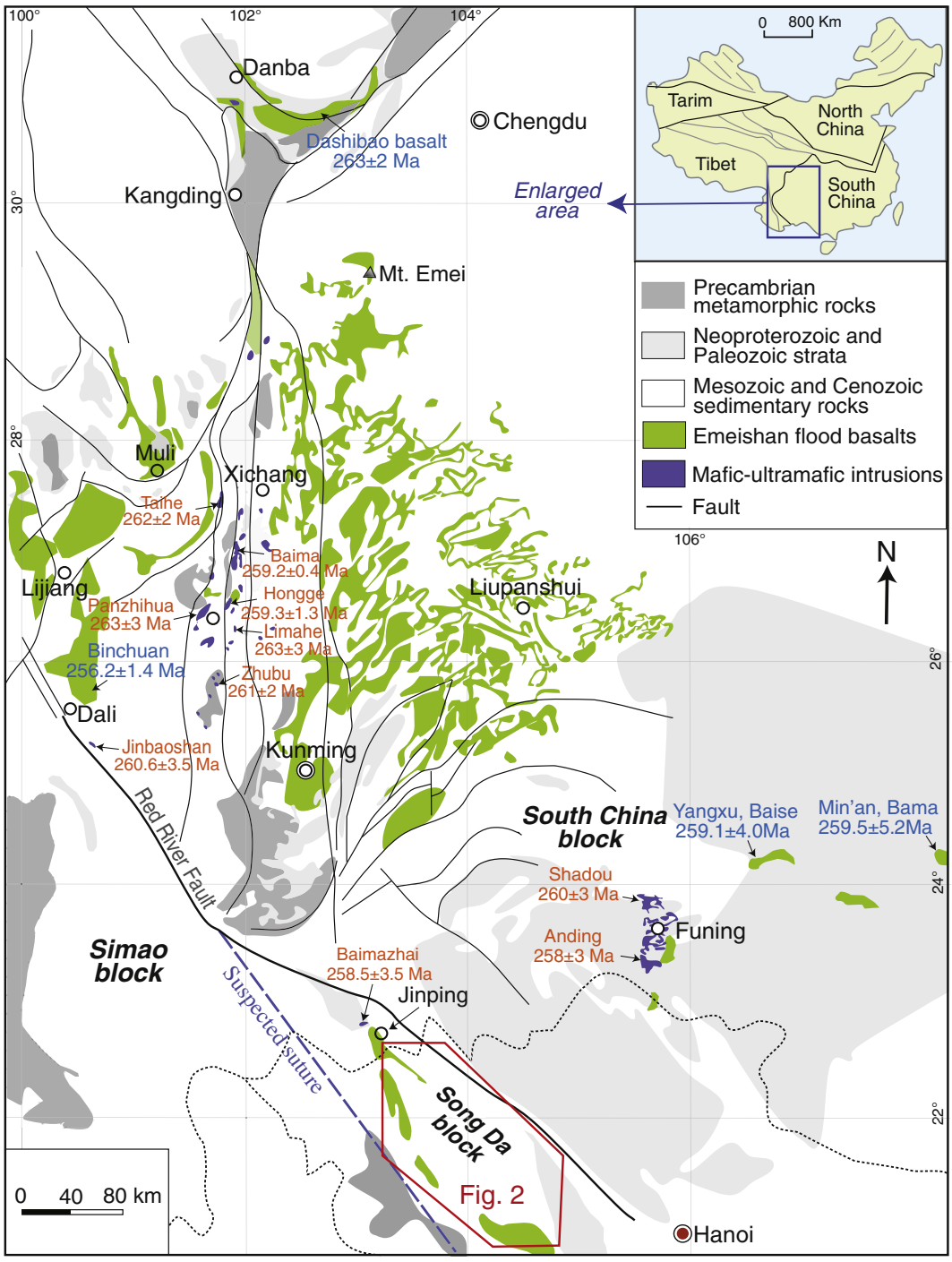

Fig. 1. Distribution of the Emeishan flood basalt province and coeval mafic–ultramafic intrusions (after Tang et al., 2015). The suspected suture is from Chung et al. (1997) and Wang et al. (2014). The zircon U–Pb ages are from Fan et al. (2008), Shellnutt et al. (2011, 2012), Tao et al. (2009), Tang et al. (2015), Wang et al. (2006), Zhong and Zhu (2006), Zhou et al. (2002, 2005, 2006, 2008), Zi et al. (2010).

elements to compare basalts and picrites in the Emeishan province. In particular, we evaluate the effects of mantle source variation, fractional crystallization and crustal contamination on PGE fractionation in natural basaltic systems related to a single mantle plume.

2. The Emeishan flood basalt province

Voluminous flood basalts in southwest China are commonly referred to as the Emeishan flood basalt province (Fig. 1). The ages of the Emeishan flood basalts were originally inferred from the U–Pb ages of zircon from the coeval mafic–ultramafic intrusions in the region (~260 Ma, Zhou et al., 2002). This has now been confirmed by the U–Pb ages of zircon from the associated volcanic rocks (Fan et al., 2008; Tang et al., 2015; Zi et al., 2010).

Permian flood basalts are also present in the Song Da district, northern Vietnam (Fig. 1). Based on geological and petrological correlations, Chung et al. (1997) suggested that the basalts in this region are part of the Emeishan flood basalt province. The large distance between this

occurrence and those in SW China is due to the ~700 km left-lateral movement along the Red River fault in the Cenozoic during the Himalaya orogeny (Leloup et al., 1995; Tapponnier et al., 1990). In the Song Da district, no U–Pb zircon ages have been reported for the Permian basalts or coeval mafic–ultramafic intrusions including the Ban Phuc intrusion which hosts a magmatic Ni–Cu sulfide deposit (Glotov et al., 2001), but the spatially associated rhyolites yield a mean U–Pb zircon age of 259.8 ± 3.1 Ma (Fig. 2, Usuki et al., 2015), which is indistinguishable with the U–Pb zircon ages of the Permian Emeishan basalts in SW China (~260 Ma, Fan et al., 2008; Tang et al., 2015; Zi et al., 2010).

The Permian flood basalt sequence in the Emeishan flood basalt province has a thickness varying from several hundred meters up to 5000 m (Anh et al., 2011; Chung and Jahn, 1995; Hanski et al., 2004; Xiao et al., 2004; Xu et al., 2001). Minor picrites are present at several locations such as Ertan in Sichuan province, Dali and Lijiang in Yunnan province, and Son La in northern Vietnam (Fig. 1).

3. Sampling and analytical methods

3.1. Samples

The new samples used in this study were collected along several major roads (no. 6, 37 and 107) in the vicinity of Son La city (Fig. 2). A total of 11 samples were collected: 1 picrite, 8 basalts and 2 andesites. The coordinates of these samples are listed within Fig. 2. The footwall and hanging-wall of the volcanic succession at this location are Carboniferous and Triassic sedimentary rocks, respectively (Anh et al., 2011). Three picrite flows with thicknesses varying from 1.5 to 3 m occur in the lower part of the volcanic succession (Anh et al., 2011). Our picrite sample (SL-6) is from the uppermost flow. Like elsewhere in the Emeishan flood basalt province (e.g., Tang et al., 2015), the picrite flow stands out in the outcrop (Fig. 3a) due to its greater resistance to weathering than the associated basaltic flows.

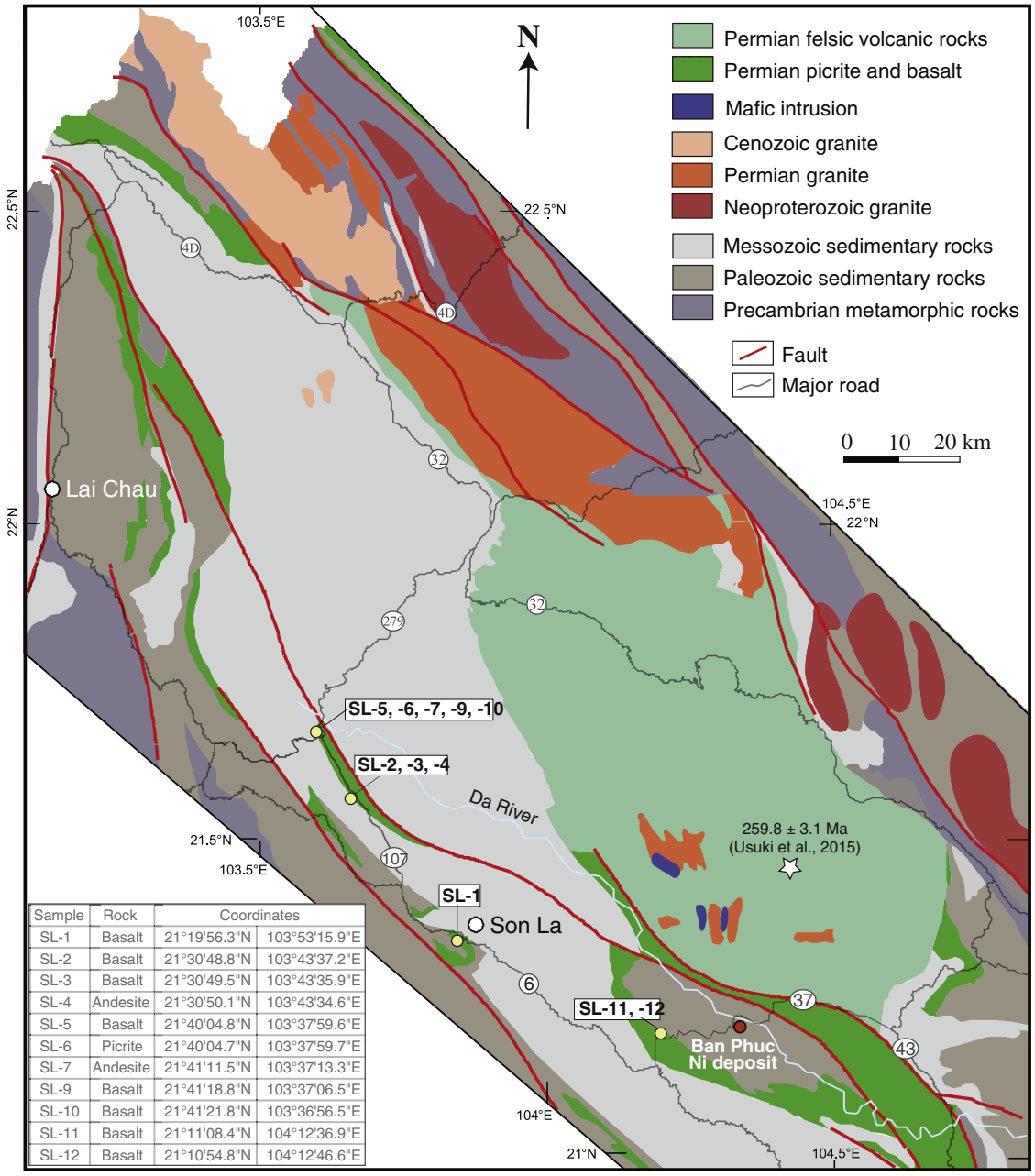

Sample	Rock	Coordinates	
SL-1	Basalt	21°19'56.3"N	103°53'15.9"E
SL-2	Basalt	21°30'48.8"N	103°43'37.2"E
SL-3	Basalt	21°30'49.5"N	103°43'35.9"E
SL-4	Andesite	21°30'50.1"N	103°43'34.6"E
SL-5	Basalt	21°40'04.8"N	103°37'59.6"E
SL-6	Picrite	21°40'04.7"N	103°37'59.7"E
SL-7	Andesite	21°41'11.5"N	103°37'13.3"E
SL-9	Basalt	21°41'18.8"N	103°37'06.5"E
SL-10	Basalt	21°41'21.8"N	103°36'56.5"E
SL-11	Basalt	21°11'08.4"N	104°12'36.9"E
SL-12	Basalt	21°10'54.8"N	104°12'46.6"E

Fig. 2. Distribution of Permian basalt–picrite lavas in the Song Da zone, northern Vietnam (modified from Anh et al., 2011; Usuki et al., 2015), with sample locations.

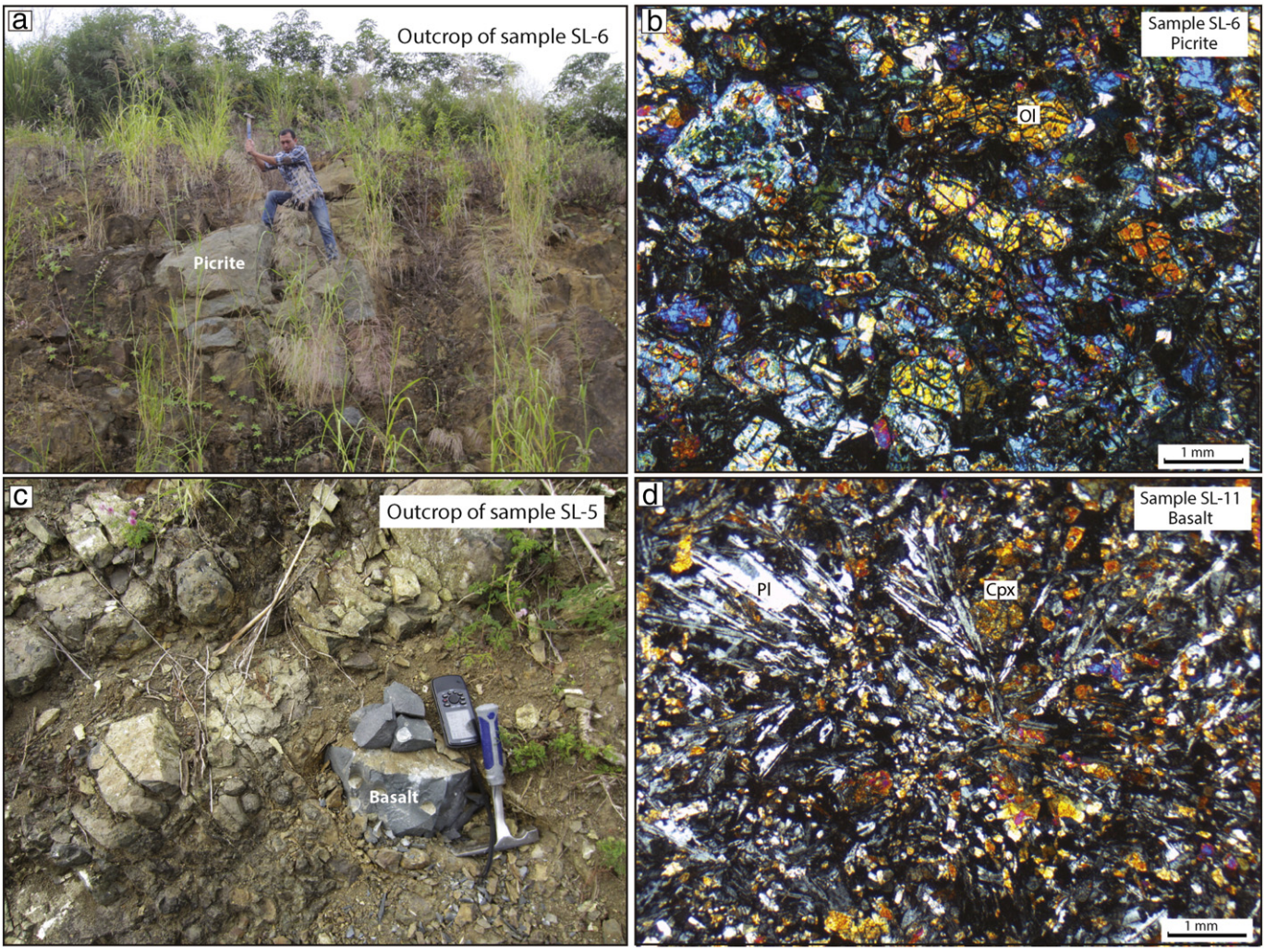

Fig. 3. Photos of outcrops and photomicrographs of representative picrite and basalt from Song Da district, northern Vietnam. Cpx = clinopyroxene, Pl = plagioclase, Ol = olivine.

The picrites from the Son La area, Song Da district, Vietnam contain abundant olivine phenocrysts with grain sizes varying from 0.5 to 2 mm across, plus rare, smaller clinopyroxene phenocrysts (Fig. 3b). Small Cr–spinel inclusions are present in some large olivine phenocrysts. Serpentine alteration is commonly present in the margins and micro-fractures of olivine phenocrysts. The groundmasses of the picrites are composed of fine-grained pyroxene, plagioclase and spinels, and their alteration products.

The basaltic samples contain 5–15 vol% clinopyroxene or plagioclase phenocrysts. These volcanic rocks are commonly characterized by aphanitic and amygdaloidal textures. Ophitic texture (Fig. 3d) is rare. Variable saussuritization is present in the samples containing plagioclase.

3.2. Analytical methods

The compositions of Cr–spinel, olivine and clinopyroxene were determined by wavelength-dispersive X-ray emission microanalysis using a CAMECA SX50 electron microprobe in the Department of Geological Sciences, Indiana University, USA. Analytical conditions for major elements were 15 keV accelerating voltage, 20 nA beam current, 1 μm beam size and peak counting time of 20 s. Calcium and Ni in olivine were analyzed using a beam current of 100 nA and a peak counting time of 100 s. Under these conditions the detection limits were estimated to be 20 ppm Ca and 80 ppm Ni by counting statistics. International standards were used for calibration. Matrix effects were corrected using the PAP program supplied by CAMECA. Analytical uncertainty is within ±2% of accepted values, based on the results from the San Carlos olivine standard (USNM 1113122/444) analyzed together with our samples.

Major element abundances in whole-rocks were determined on fused glass discs using an AXIOS-PW4400 X-ray fluorescence (XRF) instrument in the State Key Laboratory of Ore Deposit Geochemistry, Institute of Geochemistry, Chinese Academy of Sciences, Guiyang, China. The loss-on-ignition (LOI) was determined by the weight loss of a powdered sample after one-hour heating at 100 °C. The sample powders, 1.2 g for each sample, were fused with 6 g lithium tetraborate at 1050 °C for 20 min. The accuracy was monitored using a Chinese national standard (GSR3). The standard deviations for the standard analyzed by us are generally better than 2%.

Trace element concentrations in whole rocks were analyzed using a Perkin-Elmer Sciex ELAN DRC-e quadrupole inductively coupled plasma mass spectrometry (ICP-MS) in the State Key Laboratory of Ore Deposit Geochemistry, Institute of Geochemistry, Chinese Academy of Sciences, Guiyang, China. 50 g of powders for each sample were dissolved using a mixture of HF and HNO_3 in high-pressure Teflon bomb for 48 h at 190 °C. Rh was used to monitor signal drift during data acquisition. The international standards GBPG-1 and OU-6, and the Chinese national standards GSR-1 and GSR-3, were used to monitor accuracy. The differences between our results and the recommended values for the standards are generally better than 10%.

Pt, Pd, Rh, Ru and Ir were measured by isotope dilution ICP-MS in the State Key Laboratory of Ore Deposit Geochemistry, Institute of

Geochemistry, Chinese Academy of Sciences, Guiyang, China following the procedures of Qi et al. (2011). The average values of five total procedural blanks were lower than 0.003 ppb for Ir, Ru and Rh; 0.02 ppb for Pd; and 0.011 ppb for Pt (Qi et al., 2011). The detection limits were estimated to be 0.0002 ppb for Os, 0.001 ppb for Ir, Ru and Rh, 0.009 for Pt and 0.015 for Pd based on counting statistics (Qi et al., 2011). The international standards WGB-1 (gabbro) and TDB-1 (diabase) were analyzed together with our samples to monitor accuracy. The differences between our results and the values recommended by Qi et al. (2011) for these standards are less than 20%.

Sr and Nd isotopes in whole rocks were determined using a Triton thermal ionization mass spectrometer in the State Key Laboratory of Ore Deposit Geochemistry, Institute of Geochemistry, Chinese Academy of Sciences, Guiyang, China. The sample powders were spiked with mixed isotope tracers, and then dissolved in Teflon capsules with $HF + HNO_3$. Rare earth elements and Sr were separated on the Eichrom columns with 0.1% HNO_3 as elutant. Separation of Nd from other rare earth elements was done using the HDEHP columns with 0.18 N HCl as elutant. Mass fractionation corrections for Sr and Nd isotopic ratios were based on $^{86}Sr/^{88}Sr = 0.1194$ and $^{146}Nd/^{144}Nd = 0.7219$. We used international isotope standards to monitor analytical accuracy. The average isotopic ratios of the international standards analyzed together with our samples are $^{87}Sr/^{86}Sr = 0.705018$ for the NBS-987 Sr isotope standard (the recommended value is 0.705), and $^{143}Nd/^{144}Nd = 0.51261$ for the BCR-1 Nd isotope standard (the recommended value is 0.512636).

4. Analytical results

4.1. Mineral chemistry

The compositions of olivine phenocrysts in a picrite sample from Son La, northern Vietnam (Fig. 3b), Cr–spinel inclusions in the olivine phenocrysts and clinopyroxene phenocrysts in the associated basalts (Fig. 3d) are given as supplementary data (Table S1). The contents of Fo in the cores and rims of olivine phenocrysts in the picrite sample from this location are 85–88 mol% and 82–87 mol%, respectively (Fig. 4). The Fo, Ni, Mn and Ca contents of olivine phenocrysts in the picrites from Son La, northern Vietnam and elsewhere in the Emeishan flood basalt province are comparable (Fig. 4). The Cr number [$Cr^{\#} = Cr/(Cr + Al)$, molar] of Cr–spinel inclusions enclosed in olivine phenocrysts in the picrite from Son La, northern Vietnam are from 0.48 to 0.51, which overlap the lower end of the values (0.5–0.79) for the Cr–spinel inclusions enclosed in olivine phenocrysts in the picrites from elsewhere in the Emeishan flood basalt province (Hanski et al., 2010; Li et al., 2008). The Mg-number [or $Mg^{\#} = 100MgO/(MgO + FeO^{Total})$, molar] of clinopyroxene phenocrysts in a basaltic sample from Son La, northern Vietnam vary from 80 to 82, which are similar to the values of clinopyroxene phenocrysts in basalts from elsewhere in the Emeishan flood basalt province (Tao et al., 2015).

4.2. Lithophile elements

The concentrations of major and trace lithophile elements in the Son La volcanic rocks are listed in Table 1. The basaltic samples are further divided into alkaline and subalkaline groups based on the classification (i.e., $Na_2O + K_2O$ versus SiO_2) of Irvine and Baragar (1971). The mantle-normalized immobile trace element patterns of the volcanic rocks from Son La, northern Vietnam are illustrated in Fig. 5. The picrite sample from this location is characterized by light REE depletions relative to heavy REE. A subalkaline basalt sample from this location is characterized by moderate enrichments in light REE. Both enrichments and depletions in light REE are present in the alkaline basalts from this location. The picrite sample and two of five alkaline basalt samples from this location show a moderate negative Nb anomaly.

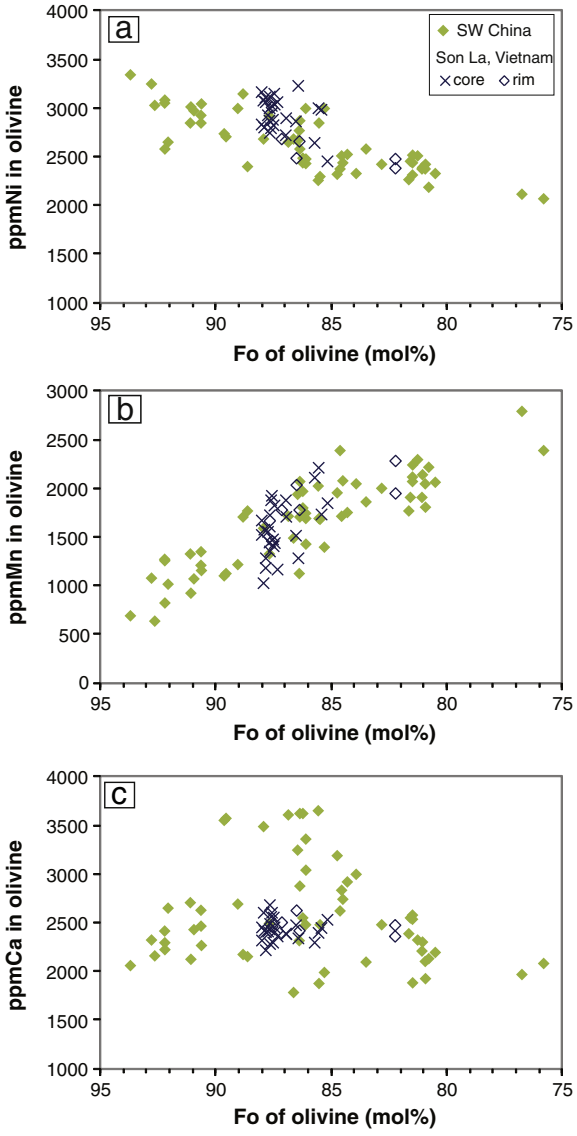

Fig. 4. Compositional variations of olivine phenocrysts in picrites from the Emeishan flood basalt province. Data for the samples from SW China and Son La, northern Vietnam are from Li et al. (2012) and this study, respectively.

Available data for the entire Emeishan flood basalt province (see summary in Li et al., 2012) indicate that depletions in light REE in picrites and some basalts are restricted to the Song Da zone in northern Vietnam and the northern extension of this zone in the Jinping country, Yunnan province, China (see Fig. 1 for the locations).

4.3. Ni, Cu and platinum-group elements

The concentrations of Ni, Cu and PGE in the Permian volcanic rocks from Son La, northern Vietnam are listed in Table 2. The mantle-normalized chalcophile element patterns for these rocks are illustrated in Fig. 6. The mantle-normalized PGE patterns of picrites from this location and elsewhere in the Emeishan flood basalt province are similar (Fig. 6). The associated basalts and andesites from Son La, northern Vietnam are characterized by more fractionated PGE patterns. Two basaltic samples (plus another not shown) from Son La, northern Vietnam are significantly depleted in PGE (Fig. 6). No systematic variations in PGE compositions are found between the alkaline and subalkaline varieties at this location, similar to the observation for the basalts in other parts of the Emeishan flood basalt province (Li et al., 2012).

Table 1
Whole-rock major and trace element compositions, Permian volcanic rocks from Son La, Vietnam.

Sample	SL-7	SL-11	SL-6	SL-1	SL-2	SL-3	SL-4	SL-5	SL-9	SL-10	SL-12
Rock type	Basaltic andesite	Basalt	Picrite	Basalt	Basalt	Basalt	Andesite	Basalt	Basalt	Basalt	Basalt
Series	Subalkaline			Alkaline							
Oxides (wt.%)											
SiO_2	55.16	46.74	43.68	44.14	48.80	47.32	60.07	48.48	49.43	49.78	47.54
TiO_2	0.85	0.75	0.50	3.75	2.27	2.97	1.17	0.87	0.73	0.73	2.07
Al_2O_3	14.35	11.88	9.76	14.99	14.93	13.68	16.24	15.47	15.15	14.43	15.45
$Fe_2O_3^{Total}$	8.10	10.33	10.88	16.77	12.29	14.45	7.92	11.95	10.48	10.65	9.96
MnO	0.15	0.17	0.16	0.27	0.16	0.17	0.15	0.14	0.16	0.17	0.16
MgO	5.57	10.13	21.66	5.61	6.23	5.64	2.04	8.50	9.86	9.35	8.27
CaO	6.54	12.96	7.69	9.09	8.61	7.78	0.96	8.37	6.71	7.61	7.75
Na_2O	6.05	2.35	0.51	3.06	3.61	4.99	6.65	3.22	3.64	3.97	3.43
K_2O	0.06	0.03	0.03	1.02	1.09	0.25	2.46	0.80	0.78	0.38	1.47
P_2O_5	0.09	0.17	0.03	0.66	0.29	0.44	0.23	0.06	0.06	0.06	0.32
LOI	2.77	4.00	5.18	1.62	1.94	2.66	1.57	1.87	3.49	3.16	2.63
Total	99.69	99.52	100.08	100.98	100.23	100.34	99.46	99.73	100.50	100.29	99.05
Trace elements (ppm)											
Li	1.20	4.82	3.30	7.81	9.01	10.30	7.57	1.93	2.69	2.86	9.38
Sc	30.5	41.3	29.4	24.2	27.1	29.1	12.2	38.4	38.8	35.1	22.9
V	177	274	194	392	293	321	1.04	287	235	260	178
Cr	279	843	1575	23	161	142	1	357	541	448	311
Co	70.6	60.6	87.4	66	51.9	50.6	26.6	71.7	53.5	51.6	48.4
Ni	25	322	892	57	109	108	1	156	157	150	135
Cu	118	42	97	85	79	147	37	33	110	94	63
Zn	56.9	83	78.2	157	113	135	340	88.4	88.6	74.6	109
Ga	17.1	16.6	9.55	21.8	20	21	47.4	14.2	12.6	12.6	15.3
Rb	1.0	0.7	6.2	10.8	34.9	6.9	60.8	26.5	31.9	17.4	48.3
Sr	77.9	273	38.5	539	435	365	176	161	143	145	445
Y	22.2	14.1	13.0	28.2	27.2	31.1	60.8	21.2	18.4	18.3	19.8
Zr	140	40	24	221	193	222	809	49	56	57	176
Nb	7.6	6.1	0.5	29.8	20.9	23.7	98.0	1.3	3.6	3.8	33.6
Ba	14	35	3	656	465	98	534	136	96	55	717
La	13.8	3.8	0.8	33.3	22.7	25.9	65.1	1.8	5.8	6.9	23.9
Ce	31.2	8.5	2.3	77.5	51.6	59.1	144.0	5.2	13.6	14.8	51.0
Pr	3.5	1.0	0.4	9.7	6.1	7.2	20.5	0.8	1.6	1.7	5.7
Nd	13.4	4.7	2.1	41.2	26.2	31.1	84.2	4.0	6.8	6.8	22.9
Sm	2.92	1.33	0.82	8.11	5.62	6.90	17.50	1.74	1.83	1.82	4.49
Eu	0.88	0.51	0.45	3.27	2.03	2.63	5.78	0.75	0.60	0.61	1.57
Gd	3.22	1.68	1.39	7.26	5.55	6.66	14.55	2.44	2.19	2.30	4.35
Tb	0.62	0.34	0.30	1.10	0.88	1.07	2.48	0.48	0.45	0.46	0.70
Dy	3.73	2.25	2.08	5.60	4.78	5.61	13.40	3.22	2.87	2.93	3.66
Ho	0.78	0.50	0.46	1.10	0.93	1.12	2.64	0.73	0.65	0.64	0.71
Er	2.34	1.44	1.28	2.96	2.77	3.05	7.10	2.10	1.90	1.91	1.91
Tm	0.34	0.22	0.20	0.39	0.36	0.38	1.05	0.30	0.27	0.30	0.25
Yb	2.32	1.50	1.24	2.36	2.21	2.52	6.69	1.94	1.92	1.90	1.61
Lu	0.34	0.20	0.19	0.31	0.31	0.33	0.93	0.29	0.28	0.28	0.21
Hf	4.10	1.25	0.68	5.09	4.87	5.66	22.17	1.27	1.49	1.60	4.06
Ta	0.58	0.36	0.05	1.89	1.29	1.47	7.49	0.12	0.23	0.24	2.25
Th	5.70	0.90	0.16	3.48	2.93	3.07	18.60	0.36	1.67	1.75	2.94
U	1.05	0.19	0.05	0.34	0.73	0.85	4.46	0.11	0.37	0.35	0.56

LOI, loss on ignition. Total Fe reported as Fe_2O_3.

4.4. Sr and Nd isotopes

The Sr and Nd isotopic compositions of the Permian volcanic rocks from Son La, northern Vietnam are also given in Table 2. The calculated ε_{Nd} ($t = 260$ Ma) value and initial $^{87}Sr/^{86}Sr$ ratio for a picrite sample from this location are +5.7 and 0.70288, respectively. The ε_{Nd} values and initial $^{87}Sr/^{86}Sr$ ratios for the associated alkaline basalts are from −6 to +3.9 and from 0.7044 to 0.7095, respectively. A subalkaline basalt from this location has $\varepsilon_{Nd} = -1.45$ and initial $^{87}Sr/^{86}Sr$ ratio = 0.7059, which are within the ranges of the associated alkaline basalts from this location.

5. Data integration and discussion

In order to make the best use of our new but limited number of analyses for the picrite–basalt association in the Song Da district, northern Vietnam, we have carried out comprehensive data integration for the entire Emeishan flood basalt province. The results are given below.

5.1. The effects of alteration, crustal contamination and mantle heterogeneity

The calculated ε_{Nd} ($t = 260$ Ma) values and initial $^{87}Sr/^{86}Sr$ ratios for the Emeishan flood basalt province are highly variable (Fig. 7a). The basalts show a weak, negative correlation between ε_{Nd} and $(^{87}Sr/^{86}Sr)_i$ values. The mixing calculation shows that such correlation cannot be explained by crustal contamination alone (Fig. 7a). Hydrothermal alteration may have also contributed to the observed Sr isotope scattering, as indicated by the results from acid leaching experiments (e.g., Nobre Silva et al., 2010; Thompson et al., 2008) which demonstrated that low-temperature hydrothermal alteration has a negligible effect on Nd isotope compositions but a significant effect on Sr isotope compositions in basalts.

The involvement of crustal contamination in the evolution of the Emeishan flood basalts is also indicated by a positive correlation

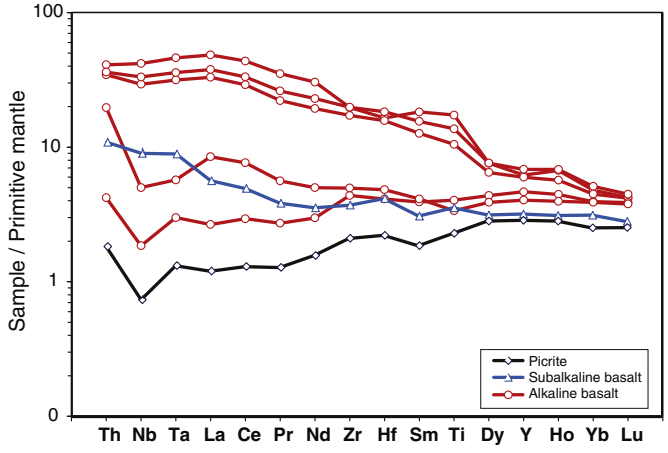

Fig. 5. Mantle-normalized immobile trace element patterns of picrite and basalts from Son La, northern Vietnam. The primitive mantle values for normalization are from Palme and O'Neill (2014).

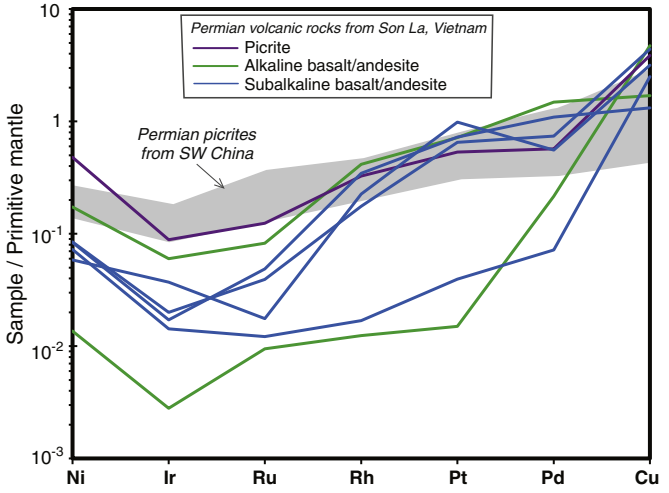

Fig. 6. Mantle-normalized Ni–Cu–PGE patterns of picrite and basalts from Son La, northern Vietnam. Data for the Permian picrites in SW China are from Li et al. (2012). The primitive mantle values for normalization are from Palme and O'Neill (2014).

between ε_{Nd} and mantle-normalized Nb/Th ratios (Fig. 7b). The Nb/Th ratio is a proxy for the degree of crustal contamination, because the continental crust is enriched in Th but depleted in Nb (see summary in Rudnick and Gao, 2014).

No correlation between ε_{Nd} and $(^{87}Sr/^{86}Sr)_i$ values is observed in the picrites from the entire Emeishan flood basalt province (Fig. 7a). The variable displacement of some picrite samples to the right of the mantle array (Fig. 7a) is consistent with the effect of post-eruption hydrothermal alteration on Sr isotope compositions in basalts (Nobre Silva et al., 2010). In contrast with the results for the associated basalts, the picrites do not show any correlation between ε_{Nd} and mantle-normalized Nb/Th ratios (Fig. 7b). This supports the interpretation that the variation of ε_{Nd} values in the picrites mainly reflects source mantle heterogeneity (Hanski et al., 2010). In Fig. 7 a picrite sample from the Song Da district given by Wang et al. (2007) was excluded, because this sample has extremely high $(^{87}Sr/^{86}Sr)_i$ (0.7132), possibly due to the occurrence of secondary calcite in the sample.

5.2. PGE fractionation during magma differentiation

Magnesium is more compatible than Fe in important minerals such as spinel, olivine and pyroxene crystallizing from high-Mg basaltic magma on cooling. As a result, the liquid Mg-number decreases as fractional crystallization proceeds. Available mineral data, and whole-rock Sr–Nd isotopes and trace element compositions together indicate that the Emeishan flood basalts are the fractionated liquids of the associated picrites (Hanski et al., 2010; Kamenetsky et al., 2012). This is further supported by lower Mg-numbers for the basalts than the associated picrites (Fig. 8).

Available chalcophile element data for the Emeishan flood basalt province show that $(Rh/Ru)_n$, $(Pt/Ru)_n$ and $(Pd/Ru)_n$ are negatively correlated with Mg-number (Fig. 8a, b, c) while $(Pt/Rh)_n$ remains constant as Mg-number changes (Fig. 8d). These indicate that Pt, Pd and Rh all behave incompatibly during fractional crystallization, which is consistent with the results from some komatiite–basalt suites in the world (e.g., Barnes and Fiorentini, 2008; Barnes et al., 2015; Said et al., 2011).

The inferred incompatible behavior for both Pt and Pd in basaltic systems is consistent with available experimental data (Brenan et al., 2003, 2005, 2012; Capobianco and Drake, 1990; Capobianco et al., 1994; Park et al., 2012; Righter et al., 2004). However, the inferred incompatible behavior for Rh in basaltic systems is at odds with the experimental results. New experiments are required to solve this mystery.

5.3. Origin of Pt–Pd depletion

The main reason for Pd–Pt–Cu depletions in basalts as compared to coexisting picrites in a given flood basalt province is generally thought

Table 2
PGE concentrations and Sr–Nd isotope compositions, Permian volcanic rocks from Son La, Vietnam.

Sample	SL-7	SL-11	SL-6	SL-1	SL-2	SL-3	SL-4	SL-5	SL-9	SL-10	SL-12
Rock type	Basaltic andesite	Basalt	Picrite	Basalt	Basalt	Basalt	Andesite	Basalt	Basalt	Basalt	Basalt
Series	Subalkaline			Alkaline							
Ni and Cu, ppm											
Ni	25	322	892	57	109	108		156	157	150	135
Cu	118	42	97	85	79	147	37	33	110	94	63
PGE, ppb											
Ir	0.01	0.21	0.31		0.13	0.19	0.03	0.06	0.07	0.06	0.05
Ru	0.07	0.61	0.92		0.13	0.19	0.07	0.36	0.29	0.29	0.09
Rh	0.01	0.50	0.39		0.27	0.22	0.01	0.41	0.21	0.12	0.02
Pt	0.11	5.47	4.05		7.51	4.83	0.07	5.50	4.95	5.24	0.30
Pd	1.53	10.54	4.05		3.95	4.47	2.44	7.78	5.27	5.55	0.51
Sr–Nd isotopes											
$^{87}Sr/^{86}Sr$		0.705970	0.704599	0.705496	0.706107	0.706121	0.709413	0.706153	0.710685	0.710751	0.706392
$^{143}Nd/^{144}Nd$		0.512522	0.512996	0.512532	0.512576	0.512581	0.512539	0.512947	0.512272	0.512266	0.512507
$(^{87}Sr/^{86}Sr)i$		0.705942	0.702882	0.705282	0.705250	0.705918	0.705724	0.704395	0.708303	0.709470	0.705233
ε_{Nd} (t = 260 Ma)		−1.45	5.72	0.51	1.02	0.96	0.43	3.91	−6.04	−6.07	0.04

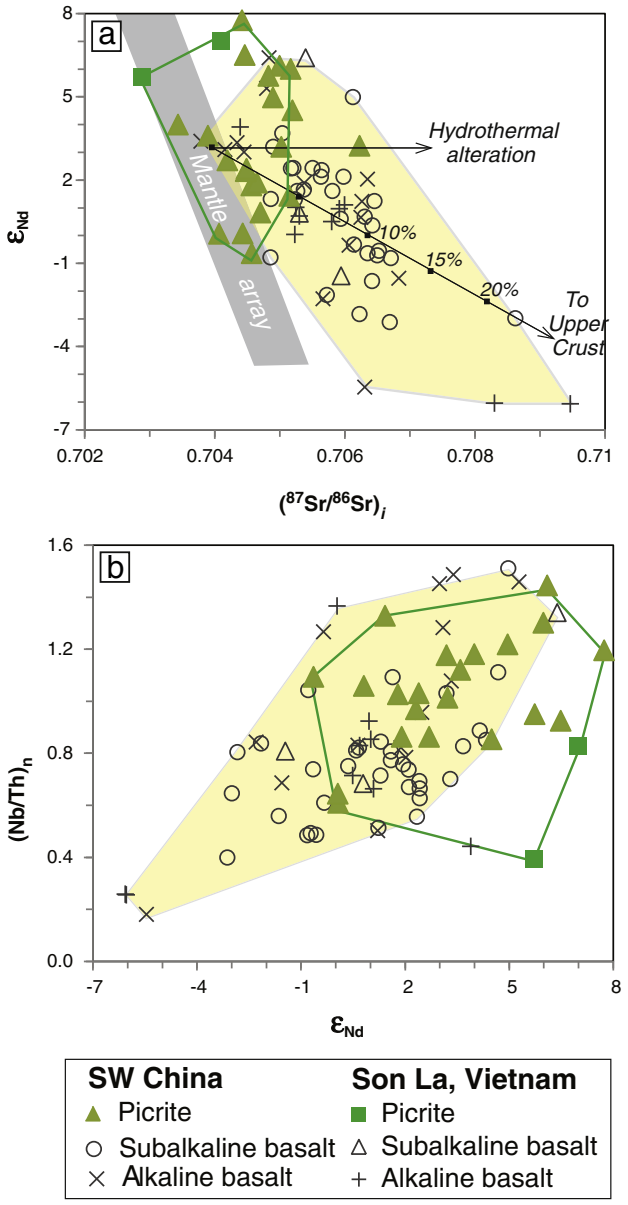

Fig. 7. Relationships between ε_{Nd}, initial $^{87}Sr/^{86}Sr$, and mantle-normalized Nb/Th ratios of whole rock samples from the Emeishan flood basalt province. Data are from this study and previous publications (Bai et al., 2013; Li et al., 2010, 2014; Li et al., 2012; Qi and Zhou, 2008; Qi et al., 2008; Song et al., 2006, 2008, 2009; Wang et al., 2007; Xiao et al., 2004; Zhang et al., 2005, 2006). The mantle Sr–Nd isotope array is from Hart and Zindler (1986). The primitive mantle values for normalization are from Palme and O'Neill (2014).

to be related to segregation of immiscible sulfide liquid from magma (e.g., Lightfoot and Keays, 2005). This is because these elements are incompatible during factional crystallization of important phases such as Cr–spinel and olivine but strongly partition into immiscible sulfide liquid. Experimental results have showed that the partition coefficients between sulfide liquid and silicate melt for Pd and Pt are much higher than that for Cu, i.e., ~10^5 for Pt and Pd (Mungall and Brenan, 2014) and ~10^3 for Cu (Peach et al., 1990; Ripley et al., 2002). As a result, the removal of immiscible sulfide liquid from magma can cause more severe depletions of Pt and Pd than Cu in the magma. Hence, a plot of Pd (or Pt) versus Cu is particularly useful in detecting Pd depletion due to sulfide removal from magma (Vogel and Keays, 1997). This type of plot (Fig. 9a) shows that some basalts (both alkaline and subalkaline series) from the Emeishan flood basalt province are significantly depleted in Pd as compared to the associated picrites, indicating sulfide segregation from the parent magma of the basaltic samples. One of the Pd-depleted basaltic samples shows no sign of Cu depletion, possibly due to Cu addition during post-eruption hydrothermal alteration. The data for the entire flood basalt province also show that some basaltic samples contain higher Cu as well as Pd than the associated picrites (Fig. 9a), and is consistent with the result of fractional crystallization during which both elements behave similarly.

The Pd-depleted samples are characterized by Pd × 10^5/Yb close to 100 (Fig. 9b). The lower limit of the Mg-number for the Pd-depleted basalts is smaller than the minimum value for the undepleted basalts whereas the upper limit of Mg-number for the Pd-depleted basalts is similar to the maximum value for the undepleted basalts. This indicates that fractional crystallization did not play a major role in triggering sulfide saturation in the magma.

As described above (Fig. 7b), the positive correlation between ε_{Nd} and $(Nb/Th)_n$ in the Emeishan basalts indicates that these values are good indexes for crustal contamination. As shown in the plots of Pd × 10^5/Yb versus ε_{Nd} and $(Nb/Th)_n$ (Fig. 9c, d), the Pd-depleted basalts are among those with relatively low ε_{Nd} and $(Nb/Th)_n$ values in the province. This indicates that crustal contamination played a role in triggering sulfide saturation in the parent magmas of the Pd-depleted basaltic samples. The decreases in both ε_{Nd} and $(Nb/Th)_n$ values are mainly due to addition of siliceous materials from the continental crust. The fact that not all of the lavas with low ε_{Nd} and $(Nb/Th)_n$ values are depleted in Pd (Fig. 9c, d) indicates that siliceous contamination alone did not cause sulfide saturation in the magma. Based on the results from the Siberian and Deccan flood basalt provinces, Keays and Lightfoot (2010) suggested that the addition of crustal sulfur is critical in triggering significant sulfide oversaturation in continental flood basalts. The data from the Emeishan flood basalt province are consistent with the combination of siliceous contamination and the addition of external sulfur being important in inducing sulfide saturation in the magma. New S–Os isotopes and S/Se ratios for the basalts are needed for further discrimination between these processes.

5.4. A possible Ir-depleted mantle component

The picrites from the entire Emeishan flood basalt province show no systematic variation between the mantle-normalized Pt/Ru and La/Yb for the entire province (Fig. 10a). Within the entire province only the picrites from Son La, northern Vietnam are characterized by Ir depletion relative to Ru (Fig. 10b). These picrites also have low mantle-normalized La/Yb (0.2–2.4) and high Al_2O_3/TiO_2 (>12, Fig. 10c). No picrite from elsewhere in the province shows the combination of these characteristics. Since the depletion of Ir relative to Ru is present most commonly in a fertile lherzolite mantle component (Becker et al., 2006), the Ir depletion in the picrites from Son La, northern Vietnam may be considered as evidence for the involvement of such component in magma generation at this particular location. However, this interpretation is tenuous, because it is based on limited number of analyses.

6. Conclusions

Important messages from this synthesis based on previously published data for the Emeishan flood basalt province plus new data from the southernmost part of the province are listed below.

(1) Correlations between ε_{Nd}, $(^{87}Sr/^{86}Sr)_i$ and $(Nb/Th)_n$ are present in the basalts but not in the associated picrites, indicating that crustal contamination is negligible in the picrites but significant in some of the basalts.
(2) Negative correlations between $(Rh/Ir)_n$, $(Pt/Ru)_n$, $(Pd/Ru)_n$ and Mg-number indicate that Ru behaves compatibly whereas Rh, Pt and Pd behave incompatibly during fractional crystallization of the lavas, which is consistent with experimental results.

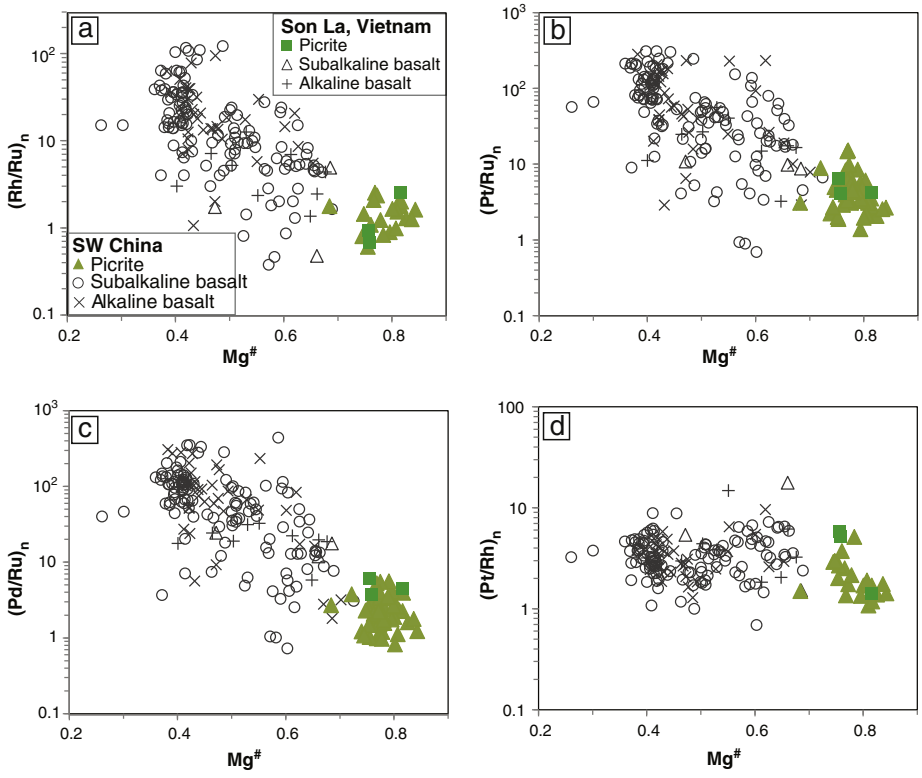

Fig. 8. Relationships between mantle-normalized PGE ratios and Mg-number [$Mg^{\#} = (MgO/FeO^{Total})$, molar] of whole rock samples from the Emeishan flood basalt province.

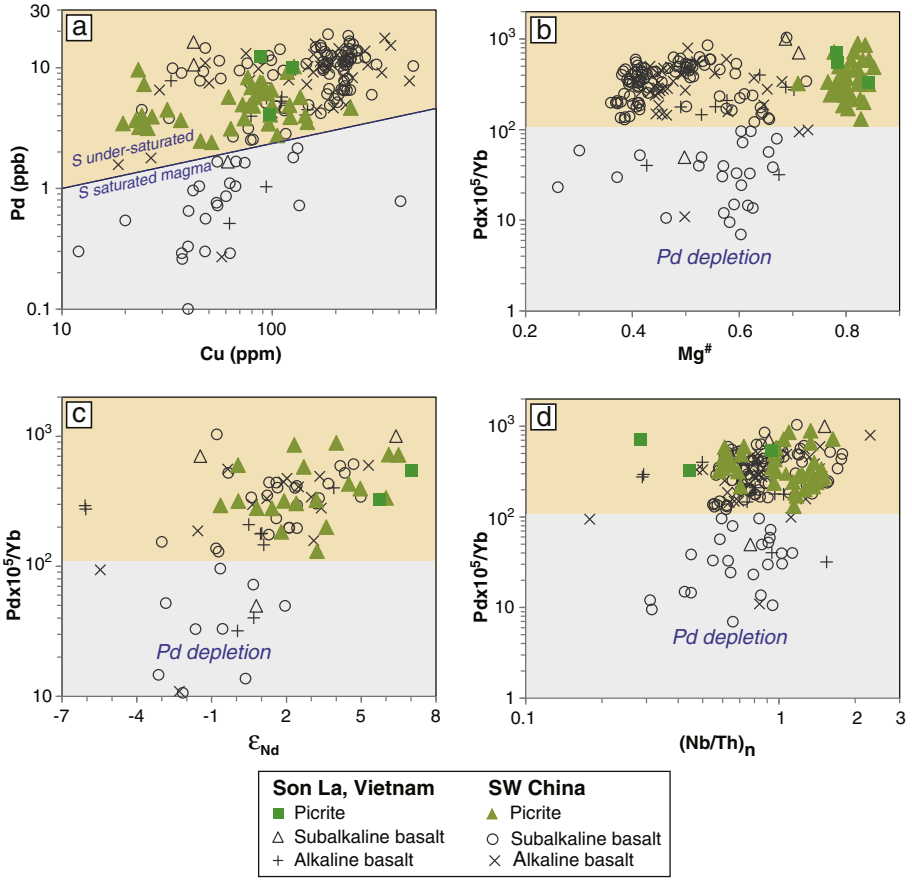

Fig. 9. Relationships between Pd and Cu contents, 10^5Pd/Yb, $Mg^{\#}$, ε_{Nd} and mantle-normalized Nb/Th ratios of whole rock samples from the Emeishan flood basalt province. The empirical Pd–Cu division for S under-saturated and saturated basalts is from Vogel and Keays (1997).

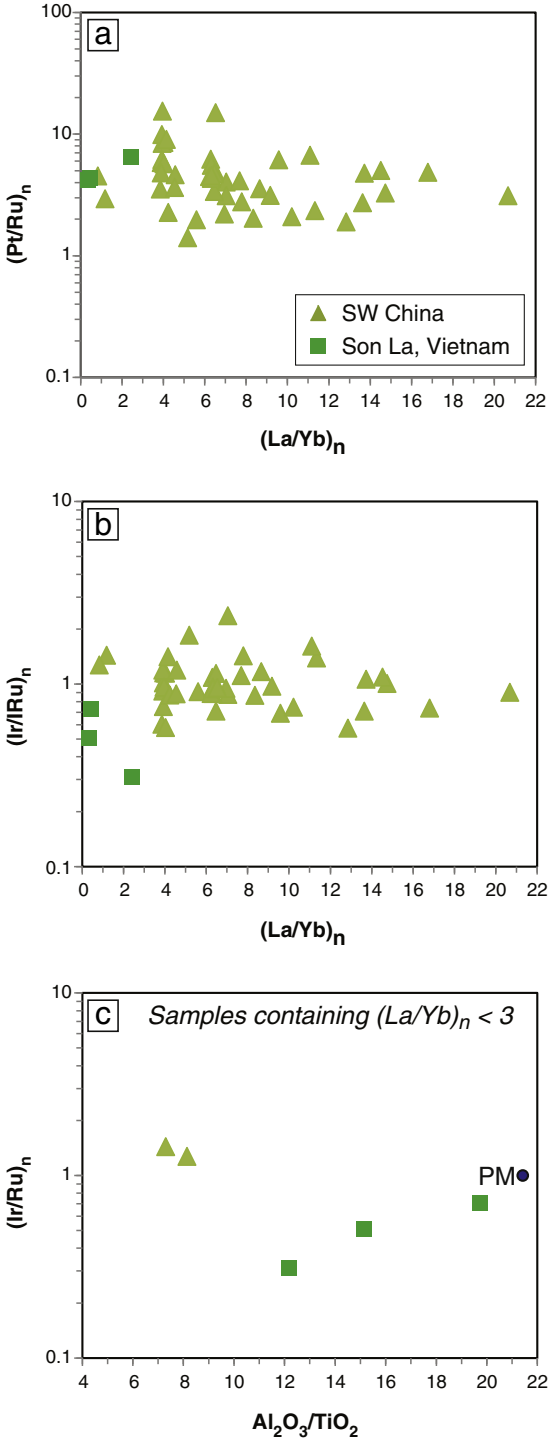

Fig. 10. Relationships between selected PGE and lithophile element ratios. The primitive mantle values for normalization are from Palme and O'Neill (2014).

(3) The incompatible behavior of Rh during fractional crystallization of basaltic magmas in nature, which is inconsistent with available experiments, is further supported by the fact that $(Pt/Rh)_n$ in the natural samples remains constant as Mg-number changes.
(4) Depletions of Pd and Pt, and to a lesser degree Cu, in some basaltic samples that have relatively low ε_{Nd} and $(Nb/Th)_n$ confirm that crustal contamination including addition of external sulfur played a critical role in triggering sulfide saturation in the parent magmas of these samples.
(5) In the Emeishan province only the picrites from northern Vietnam are clearly depleted in Ir relative to Ru; these samples are also characterized by high Al_2O_3/TiO_2 (>12) and low mantle-normalized La/Yb (0.2–2.4), possibly due to the involvement of an Ir-depleted, fertile lherzolite mantle component in magma generation at this particular location.

Acknowledgments

This study was financially supported by the CAS/SAFEA International Partnership Program for Creative Research Teams (Intraplate Mineralization Research Team, KZZD-EW-TZ-20), National 973 Research Program of China (2015CB452600) and the Natural Science Foundation of China (41473051). We thank Minh and Arndt Schimmelmann, and Tran Viet Anh for field assistance, and Feng Xiong for PGE and isotope analysis. Constructive reviews by two anonymous reviewers and useful guidance from the editor are greatly appreciated.

Appendix A. Supplementary data

Supplementary data to this article can be found online at http://dx.doi.org/10.1016/j.lithos.2015.12.027.

References

Anh, T.V., Pang, K.-N., Chung, S.-L., Lin, H.-M., Hoa, T.T., Anh, T.T., Yang, H.-J., 2011. The Song Da magmatic suite revisited: a petrologic, geochemical and Sr–Nd isotopic study on picrites, flood basalts and silicic volcanic rocks. Journal of Asian Earth Sciences 42, 1341–1355.
Bai, M., Zhong, H., Zhu, W., Bai, Z., He, D., 2013. Platinum-group element geochemical characteristics of the picrites and high-Ti basalts in the Binchuan area, Yunnan province. Acta Geologica Sinica 87, 158–175.
Barnes, S.J., Fiorentini, M.L., 2008. Iridium, ruthenium and rhodium in komatiites: evidence for iridium alloy saturation. Chemical Geology 257, 44–58.
Barnes, S.J., Mungall, J.E., Maier, W.D., 2015. Platinum group elements in mantle melts and mantle samples. Lithos 232, 395–417.
Becker, H., Horan, M.F., Walker, R.J., Gao, S., Lorand, J.-P., Rudnick, R.L., 2006. Highly siderophile element composition of the Earth's primitive upper mantle: constraints from new data on peridotite massifs and xenoliths. Geochimica et Cosmochimica Acta 70, 4528–4550.
Brenan, J.M., McDonough, W.F., Dalpe, C., 2003. Experimental constraints on the partitioning of rhenium and some platinum-group elements between olivine and silicate melt. Earth and Planetary Science Letters 212, 135–150.
Brenan, J.M., McDonough, W.F., Ash, R., 2005. An experimental study of the solubility and partitioning of iridium and osmium between olivine and silicate melt. Earth and Planetary Science Letters 237, 855–872.
Brenan, J.M., Finnigan, C.F., McDonough, W.F., Homolova, V., 2012. Experimental constraints on the partitioning of Ru, Rh, Ir, Pt and Pd between chromite and silicate melt: the importance of ferric iron. Chemical Geology 302–303, 16–32.
Capobianco, C.H., Drake, M., 1990. Partitioning of ruthenium, rhodium, and palladium between spinel and silicate melt and implications for platinum-group element fractionation trends. Geochimica et Cosmochimica Acta 54, 869–874.
Capobianco, C.H., Hervig, R.L., Drake, M., 1994. Experiments on crystal/liquid partitioning of Ru, Rh and Pd for magnetite and hematite solid solutions crystallized from silicate melt. Chemical Geology 113, 23–43.
Chung, S.-L., Jahn, B.-M., 1995. Plume–lithosphere interaction ingeneration of the Emeishan flood basalts at the Permian–Triassic boundary. Geology 23, 889–892.
Chung, S.-L., Lee, T.-Y., Lo, C.-H., Wang, P.-L., Chen, C.-Y., Yem, N.T., Hoa, T.T., Wu, G., 1997. Intraplate extension prior to continental extrusion along the Ailao Shan–Red River shear zone. Geology 25, 311–314.
DePaolo, D.J., 1981. Trace element and isotopic effects of combined wallrock assimilation and fractional crystallization. Earth and Planetary Science Letters 53, 189–202.
DePaolo, D.J., Wasserburg, G.J., 1976. Inferences about magma sources and mantle structure from variations of $^{143}Nd/^{144}Nd$. Geophysical Research Letters 3, 743–746.
Fan, W., Zhang, C., Wang, Y., Guo, F., Peng, T., 2008. Geochronology and geochemistry of Permian basalts in western Guangxi Province, southwest China: evidence for plume–lithosphere interaction. Lithos 102, 218–236.
Fiorentini, M.L., Barnes, S.J., Lesher, C.M., Heggie, G.J., Keays, R.R., Burnham, O.M., 2010. Platinum group element geochemistry of mineralized and nonmineralized komatiites and basalts. Economic Geology 105, 795–823.
Gaetani, G.A., Grove, T.L., 1997. Partitioning of moderately siderophile elements among olivine, silicate melt, and sulfide melt: constraints on core formation in the Earth and Mars. Geochimica et Cosmochimica Acta 61, 1829–1846.
Glotov, A.I., Polyakov, G.V., Hoa, T.T., Balykin, P.A., Akimtsev, V.A., Krivenko, A.P., Tolstykh, N.D., 2001. The Ban Phuc Ni–Cu–PGE deposit related to the Phanerozoic komatiite–basalt association in the Song Da rift, northwestern Vietnam. Canadian Mineralogist 39, 573–589.

Hamlyn, P.R., Keays, R.R., 1986. Sulfur saturation and second-stage melts: application to the Bushveld platinum metal deposits. Economic Geology 81, 1431–1445.
Hanski, E., Walker, R.J., Huhma, H., Polyakov, G.V., Balykin, P.A., Trong, H.T., Thi, P.N., 2004. Origin of the Permo–Triassic komatiites, northwestern Vietnam. Contributions to Mineralogy and Petrology 147, 453–469.
Hanski, E., Kamenetsky, V.S., Luo, Z.-Y., Xu, Y.-G., Kuzmin, D.V., 2010. Primitive magmas in the Emeishan large igneous province, southwestern China and northern Vietnam. Lithos 119, 75–90.
Hart, S.R., Zindler, A., 1986. In search of a bulk-earth composition. Chemical Geology 57, 247–267.
Irvine, T.N., Baragar, W.R.A., 1971. A guide to the chemical classification of the common volcanic rocks. Canadian Journal of Earth Sciences 8, 523–548.
Jowitt, S.M., Ernst, R.E., 2013. Geochemical assessment of the metallogenic potential of Proterozoic LIPs of Canada. Lithos 174, 291–307.
Kamenetsky, V.S., Chung, S.-L., Kamenetsky, M.B., Kuzmin, D.V., 2012. Picrites from the Emeishan large igneous province SW China: a compositional continuum in primitive magmas and their respective mantle sources. Journal of Petrology 53, 2095–2113.
Keays, R.R., Lightfoot, P.C., 2010. Crustal sulfur is required to form magmatic Ni–Cu sulfide deposits: evidence from chalcophile element signatures of Siberian and Deccan Trap basalts. Minerarium Deposita 45, 241–257.
Leloup, P.H., Lacassin, R., Tapponnier, P., Schärer, U., Zhong, D.L., Liu, X.H., Zhang, L.S., Ji, S.C., Phan, T.T., 1995. The Ailao Shan–Red River shear zone (Yunnan, China), tertiary transform boundary of Indochina. Tectonophysics 251, 3–84.
Li, C., Ripley, E.M., Tao, Y., Mathez, E.A., 2008. Cr–spinel/melt and Cr–spinel/olivine nickel partition coefficients from basalts, picrites and intrusive rocks. Geochimica et Cosmochimica Acta 72, 1678–1684.
Li, J., Xu, J.-F., Suzuki, K., He, B., Xu, Y.-G., Ren, Z.-Y., 2010. Os, Nd and Sr isotope and trace element geochemistry of the Muli picrites: insights into the mantle source of the Emeishan large igneous province. Lithos 119, 108–122.
Li, C., Tao, Y., Qi, L., Ripley, E.M., 2012. Controls on PGE fractionation in the Emeishan picrites and basalts: constraints from integrated lithophile–siderophile elements and Sr–Nd isotopes. Geochimica et Cosmochimica Acta 90, 12–32.
Li, J., Wang, X.-C., Ren, Z.-Y., Xu, J.-F., He, B., Xu, Y.-G., 2014. Chemical heterogeneity of the Emeishan mantle plume: evidence from highly siderophile element abundances in picrites. Journal of Asian Earth Sciences 79, 191–205.
Lightfoot, P.C., Keays, R.R., 2005. Siderophile and chalcophile metal variations in flood basalts from the Siberian Trap, Noril'sk Region: implications for the origin of the Ni–Cu–PGE sulfide ores. Economic Geology 100, 439–462.
Lorand, J.-P., Luguet, A., Alard, O., 2008. Platinum-group elements: a new set of key tracers for the Earth's interior. Elements 4, 247–252.
Lorand, J.-P., Luguet, A., Alard, O., 2013. Platinum-group element systematics and petrogenetic processing of the continental upper mantle: a review. Lithos 164, 2–21.
Luguet, A., Shirey, S., Lorand, J.-P., Horan, M.F., Carlson, R.C., 2007. Residual platinum group minerals from highly depleted harzburgites of the Lherz massif (France) and their role in HSE fractionation of the mantle. Geochimica et Cosmochimica Acta 71, 3082–3097.
Maier, W.D., Peltonen, P., McDonald, I., Barnes, S.J., Barnes, S.-J., Hatton, C., Viljoen, F., 2012. The concentration of platinum-group elements and gold in southern African and Karelian kimberlite-hosted mantle xenoliths: implications for the noble metal content of the Earth's mantle. Chemical Geology 302, 119–135.
Mungall, J.E., Brenan, J.M., 2014. Partitioning of platinum-group elements and Au between sulfide liquid and basalt and the origins of mantle–crust fractionation of the chalcophile elements. Geochimica et Cosmochimica Acta 125, 265–289.
Nobre Silva, I.G., Weis, D., Scoates, J.S., 2010. Effects of acid leaching on the Sr–Nd–Hf isotopic compositions of ocean island basalts. Geochemistry, Geophysics, Geosystems 11, Q09011. http://dx.doi.org/10.1029/2010GC003176.
Palme, H., O'Neill, H.St.C., 2014. Cosmochemical estimates of mantle composition. In: Carlson, R.W. (Ed.), The Mantle and Core, Treatise on Geochemistry, 2nd edition Elsevier, Amsterdam, pp. 1–39.
Park, J.-W., Campbell, I.H., Eggins, S.M., 2012. Enrichment of Rh, Ru, Ir and Os in Cr spinels from oxidized magmas: evidence from the Ambae volcano, Vanuatu. Geochimica et Cosmochimica Acta 78, 28–50.
Peach, C.L., Mathez, E.A., Keays, R.R., 1990. Sulfide melt–silicate melt distribution coefficients for noble metals and other chalcophile elements as deduced from MORB: implications for partial melting. Geochimica et Cosmochimica Acta 54, 3379–3389.
Qi, L., Zhou, M.-F., 2008. Platinum-group elemental and Sr–Nd–Os isotopic geochemistry of Permian Emeishan flood basalts in Guizhou Province, SW China. Chemical Geology 248, 83–103.
Qi, L., Wang, C.Y., Zhou, M.-F., 2008. Controls on the PGE distribution of Permian Emeishan alkaline and peralkaline volcanic rocks in Longzhoushan, Sichuan Province, SW China. Lithos 106, 222–236.
Qi, L., Gao, J., Huang, X., Hu, J., Zhou, M.-F., Zhong, H., 2011. An improved digestion technique for determination of platinum group elements in geological samples. Journal of Analytical Atomic Spectrometry 26, 1900–1994.
Righter, K., Campbell, A.J., Humayun, M., Hervig, R.L., 2004. Partitioning of Ru, Rh, Pd, Re, Ir, and Au between Cr-bearing spinel, olivine, pyroxene and silicate melts. Geochimica et Cosmochimica Acta 68, 867–880.
Ripley, E.M., Brophy, J.G., Li, C., 2002. Copper solubility in a basaltic melt and sulfide liquid/silicate melt partition coefficients of Cu and Fe. Geochimica et Cosmochimica Acta 66, 2791–2800.
Rudnick, R.L., Gao, S., 2014. Composition of the continental crust. In: Rudnick, R.L. (Ed.), Treatise on Geochemistry, the Crust, 2nd edition Elsevier, Amsterdam, pp. 1–51.
Said, N., Kerrich, R., Maier, W.D., McCuaig, C., 2011. Behaviour of Ni–PGE–Au–Cu in mafic–ultramafic volcanic suites of the 2.7 Ga Kambalda Sequence, Kalgoorlie Terrane, Yilgarn Craton. Geochimica et Cosmochimica Acta 75, 2882–2910.
Shellnutt, J.G., Wang, K.-L., Zellmer, G.F., Iizuka, Y., Jahn, B.-M., Pang, K.-N., Qi, L., Zhou, M.-F., 2011. Three Fe–Ti oxide ore-bearing gabbro–granitoid complexes in the Panxi region of the Permian Emeishan large igneous province, SW China. American Journal of Science 311, 773–812.
Shellnutt, J.G., Denyszyn, S.W., Mundil, R., 2012. Precise age determination of mafic and felsic intrusive rocks from the Permian Emeishan large igneous province (SW China). Gondwana Research 22, 118–126.
Song, X.-Y., Zhou, M.-F., Keays, R.R., Cao, Z.-M., Sun, M., Qi, L., 2006. Geochemistry of the Emeishan flood basalts at Yangliuping, Sichuan, SW China: implications for sulfide segregation. Contributions to Mineralogy and Petrology 152, 53–74.
Song, X.-Y., Qi, H.-W., Robinson, P.T., Zhou, M.-F., Cao, Z.-M., Chen, L.-M., 2008. Melting of the subcontinental lithospheric mantle by the Emeishan mantle plume; evidence from the basal alkaline basalts in Dongchuan, Yunnan, Southwestern China. Lithos 100, 93–111.
Song, X.-Y., Keays, R.R., Xiao, L., Qi, H.-W., Ihlenfeld, C., 2009. Platinum-group element geochemistry of the continental flood basalts in the central Emeishan large igneous province, SW China. Chemical Geology 262, 246–261.
Tang, Q., Li, C., Zhang, M., Lin, Y., 2015. U–Pb age and Hf isotopes of zircon from basaltic andesite and geochemical fingerprinting of the associated picrites in the Emeishan large igneous province, SW China. Mineralogy and Petrology 109, 103–114.
Tao, Y., Ma, Y.S., Miao, L.C., Zhu, F.L., 2009. SHRIMP U–Pb zircon age of the Jinbaoshan ultramafic intrusion Yunnan province, SW China. Chinese Science Bulletin 54, 168–172 (in Chinese with English abstract).
Tao, Y., Putirka, K., Hu, R.-Z., Li, C., 2015. The magma plumbing system of the Emeishan large igneous province and its role in basaltic magma differentiation in a continental setting. American Mineralogist 100, 2509–2517.
Tapponnier, P., Lacassin, R., Leloup, P.H., Schaer, U., Zhong, D.L., Liu, X.H., Ji, S.C., Zhang, L.S., Zhong, J.Y., 1990. The Ailao Shan/Red River metamorphic belt: tertiary left-lateral shear between Indochina and South China. Nature 343, 431–437.
Thompson, P.M.E., Kempton, P.D., Kerr, A.C., 2008. Evaluation of the effects of alteration and leaching on Sm–Nd and Lu–Hf systematics in submarine mafic rocks. Lithos 104, 164–176.
Usuki, T., Lan, C.-T., Tran, T.H., Pham, T.D., Wang, K.-L., Shellnutt, G.J., Chung, S.-L., 2015. Zircon U–Pb ages and Hf isotopic compositions of alkaline silicic magmatic rocks in the Phan Si Pan-Tu Le region, northern Vietnam: identification of a displaced western extension of the Emeishan large igneous province. Journal of Asian Earth Sciences 97, 102–124.
Vogel, D.C., Keays, R.R., 1997. The application of platinum group geochemistry in constraining the source of basalt magmas: results from the Newer Volcanic Province, Victoria, Australia. Chemical Geology 136, 181–204.
Wang, C.Y., Zhou, M.-F., Keays, R.R., 2006. Geochemical constraints on the origin of the Permian Baimazhai mafic–ultramafic intrusion, SW China. Contributions to Mineralogy and Petrology 152, 309–321.
Wang, C.Y., Zhou, M.-F., Qi, L., 2007. Permian basalts and mafic intrusions in the Jinping (SW China)–Song Da (northern Vietnam) district: mantle sources, crustal contamination and sulfide segregation. Chemical Geology 243, 317–343.
Wang, Q., Deng, J., Li, C., Li, G., Li, Y., Qiao, L., 2014. The boundary between the Simao and Yangtze blocks and their locations in Gondwana and Rodinia: constraints from detrital and inherited zircons. Gondwana Research 26, 438–448.
Xiao, L., Xu, Y.G., Mei, H.J., Zheng, Y.F., He, B., Pirajno, F., 2004. Distinct mantle sources of low-Ti and high-Ti basalts from the Eastern Emeishan Large Igneous Province, SW China: implications for plume–lithosphere interaction. Earth and Planetary Science Letters 228, 525–546.
Xu, Y., Chung, S., Jahn, B., Wu, G., 2001. Petrologic and geochemical constraints on the petrogenesis of Permian–Triassic Emeishan flood basalts in southern China. Lithos 58, 145–168.
Zhang, Z.C., Mao, J.W., Mahoney, J.J., Wang, F., Qu, W., 2005. Platinum group elements in the Emeishan large igneous province, SW China: implications for mantle sources. Geochemical Journal 39, 371–382.
Zhang, Z.C., Mahoney, J.J., Mao, J.W., Wang, F.S., 2006. Geochemistry of picritic and associated flows of the western Emeishan flood basalt province, China. Journal of Petrology 47, 1997–2019.
Zhong, H., Zhu, W.-G., 2006. Geochronology of layered mafic intrusions from the Pan-Xi area in the Emeishan large igneous province, SW China. Mineralium Deposita 41, 599–606.
Zhou, M.-F., Malpas, J., Song, X.Y., Robinson, P.T., Sun, M., Kennedy, A.K., Lesher, C.M., Keays, R.R., 2002. A temporal link between the Emeishan large igneous province (SW China) and the end-Guadalupian mass extinction. Earth and Planetary Science Letters 196, 113–122.
Zhou, M.-F., Robinson, P.T., Lesher, C.M., Keays, R.R., Zhang, C.-J., Malpas, J., 2005. Geochemistry petrogenesis and metallogenesis of the Panzhihua gabbroic layered intrusion and associated Fe–Ti–V oxide deposits in Sichuan Province, SW China. Journal of Petrology 46, 2253–2280.
Zhou, M.-F., Zhao, J.-H., Qi, L., Su, W., Hu, R., 2006. Zircon U–Pb geochronology and elemental and Sr–Nd isotopic geochemistry of Permian mafic rocks in the Funing area, SW China. Contributions to Mineralogy and Petrology 51, 1–19.
Zhou, M.-F., Arndt, N.T., Malpas, J., Wang, C.Y., Kennedy, A.K., 2008. Two magma series and associated ore deposit types in the Permian Emeishan large igneous province, SW China. Lithos 103, 352–368.
Zi, J.-W., Fan, W.-M., Wang, Y.J., Cawood, P.A., Peng, T.-P., Sun, L.-H., Xu, Z.-Q., 2010. U–Pb geochronology and geochemistry of the Dashibao Basalts in the Songpan–Ganzi Terrane, SW China, with implications for the age of Emeishan volcanism. American Journal of Science 310, 1054–1080.
Zindler, A., Hart, S.R., 1986. Chemical geodynamics. Annual Review of Earth and Planetary Sciences 14, 493–571.